Cells From Subcutaneous Tissues Contribute to Scarless Skin Regeneration in *Xenopus laevis* Froglets

Rina Otsuka-Yamaguchi,[1] Aiko Kawasumi-Kita,[1] Nanako Kudo,[2] Yumi Izutsu,[3] Koji Tamura [ID],[1] and Hitoshi Yokoyama [ID][1,2]*

[1]Department of Developmental Biology and Neurosciences, Graduate School of Life Sciences, Tohoku University, Sendai, Japan
[2]Department of Biochemistry and Molecular Biology, Faculty of Agriculture and Life Science, Hirosaki University, Hirosaki, Japan
[3]Department of Biology, Faculty of Science, Niigata University, Niigata, Japan

Background: Mammals cannot regenerate the dermis and other skin structures after an injury and instead form a scar. However, a *Xenopus laevis* froglet can regenerate scarless skin, including the dermis and secretion glands, on the limbs and trunk after skin excision. Subcutaneous tissues in the limbs and trunk consist mostly of muscles. Although subcutaneous tissues beneath a skin injury appear disorganized, the cellular contribution of these underlying tissues to skin regeneration remains unclear. **Results**: We crossed the inbred J strain with a green fluorescent protein (GFP)-labeled transgenic *Xenopus* line to obtain chimeric froglets that have GFP-negative skin and GFP-labeled subcutaneous tissues and are not affected by immune rejection after metamorphosis. We found that GFP-positive cells from subcutaneous tissues contributed to regenerating the skin, especially the dermis, after an excision injury. We also showed that the skin on the head, which is over bone rather than muscle, can also completely regenerate skin structures. **Conclusions**: Cells derived from subcutaneous tissues, at least in the trunk region, contribute to and may be essential for skin regeneration. Characterizing the subcutaneous tissue–derived cells that contribute to skin regeneration in amphibians may lead to the induction of cells that can regenerate complete skin structures without scarring in mammals. *Developmental Dynamics 000:000–000, 2017*. © 2017 Wiley Periodicals, Inc.

Key words: Wound healing; scar; J strain; dermis; amphibian

Introduction

An intriguing feature of amphibians is their exceptional capacity to regenerate damaged organs and appendages. Urodele amphibians (newts and salamanders) can regenerate limbs as well as the lower jaw, intestine, retina, heart, tail, and spinal cord (Brockes, 1997; Straube and Tanaka, 2006; Stoick-Cooper et al., 2007; Agata and Inoue, 2012). Anuran amphibians (frogs and toads) have less regenerative capacity. For example, the *Xenopus laevis* tadpole can completely regenerate limb buds (limb primordia) amputated prior to the onset of metamorphosis, but its regenerative capacity gradually diminishes as metamorphosis progresses (Dent, 1962; Muneoka et al., 1986). After metamorphosis, the young adult *X. laevis* froglet can regenerate only an unbranched cartilaginous spike structure after limb amputation (Dent 1962; reviewed by Suzuki et al., 2006). During the early stage of limb regeneration, both urodele and anuran amphibians form a blastema, which is a group of mesenchymal progenitor cells that specifically direct the restoration of the limb. Once a blastema is established, it can form a limb autonomously, even when grafted to a different area of the body (Pietsch and Webber, 1965; Stocum, 1968; reviewed by Brockes and Kumar, 2005; Yokoyama,

2008). Since both amphibians and mammals belong to the tetrapod superclass (four-limbed vertebrates), elucidating the mechanisms of organ regeneration in amphibians may lead to new approaches in regenerative medicine to restore damaged body parts using a patient's own cells.

However, regeneration studies in amphibians have focused mostly on epimorphic regeneration (e.g., limb regeneration), and the amphibian regenerative response after a simple skin wound has rarely been studied until recently. In adult mammals, skin with an injury to the dermal layer forms collagenous scar tissue and cannot regenerate the dermis or skin derivatives such as sweat glands or hair follicles (Ferguson and O'Kane, 2004; Gurtner et al., 2008; Stocum, 2012). African spiny mice are exceptional in that they can regenerate skin as adult mammals in an autotomic manner (Seifert et al., 2012a). In skin wounds in mammals, fibroblasts migrate from subcutaneous and other nearby tissues, invade the wound, and form granulation tissue at the wound site. The migrated fibroblasts proliferate and synthesize collagens that contribute to scar formation (Broughton et al., 2006; Stocum, 2012; Yokoyama, 2008). Such scar-forming fibroblasts, called myofibroblasts, are distinguished by a marker, alpha-smooth muscle actin (α-SMA) (Gabbiani, 2003). These

*Correspondence to: Hitoshi Yokoyama, Department of Biochemistry and Molecular Biology, Faculty of Agriculture and Life Science, Hirosaki University, 3 Bunkyo-cho, Hirosaki, Aomori 036-8561, Japan. E-mail: yokoyoko@hirosaki-u.ac.jp

α-SMA-positive myofibroblasts were found not only in mammals but also in metamorphosed axolotls (Seifert et al., 2012b) and *X. laevis* frogs (Bertolotti et al., 2013). Skin regeneration without scarring is highly desirable in a clinical setting because of the many problems caused by scar tissue.

Recently, several studies have reported that amphibians can regenerate skin without scarring after a full-thickness skin wound (excision of the skin including the dermis and epidermis). Levesque et al. (2010) reported that the axolotl (*Ambystoma mexicanum*), a Mexican salamander, can regenerate its tail skin without scarring after a full-thickness skin wound. The axolotl can also regenerate its dorsal-flank skin, including the dermis and secretion glands, even after thyroxine-induced metamorphosis (Seifert et al., 2012b). Another recent study revealed that the *X. laevis* froglet (a spontaneously metamorphosed anuran amphibian) can regenerate skin on both the limb and trunk after a full-thickness skin wound (Yokoyama et al., 2011). In that study, we used the paired-type homeobox-containing transcription factor *prx1* (also called *prrx1*) (Norris et al., 2000; Ocaña et al., 2012) as a marker for limb blastema cells (Suzuki et al., 2005; Satoh et al., 2007). We also used the previously established transgenic (Tg) *X. laevis* line *Mprx1*-green fluorescent protein (GFP), which expresses GFP under the control of a 2.4-kb mouse *prx1* limb-specific enhancer (Suzuki et al., 2007), to compare limb regeneration and skin regeneration, and found that the *prx1* limb-specific enhancer was activated in both the regenerating limb and regenerating skin (Yokoyama et al., 2011). After an excisional skin wound in froglets, mononuclear cells with activated *prx1* limb-specific enhancer accumulated under the epidermis, but this enhancer was not activated in the dorsal skin of adult mice after an excisional skin injury (Yokoyama et al., 2011). Thus, we proposed that blastema-like cells with activated *prx1* limb-specific enhancer might contribute to scarless skin regeneration in the *X. laevis* froglet. Because the organization of subcutaneous tissues (primarily musculature) under a skin wound appeared disrupted, and because blastema-like cells with activated *prx1* enhancer infiltrated the musculature under and around the original wound (Yokoyama et al., 2011), we speculated that the blastema-like cells observed in scarless skin regeneration might be derived from subcutaneous tissues. Determining the cellular origin of these blastema-like cells would allow a thorough comparison of the blastemal cells involved in limb regeneration and the blastema-like cells involved in skin regeneration in amphibians, as well as between the latter cells and the scar-forming fibroblasts involved in skin wounds in mammals.

To determine the cellular origin, developmental biologists have often prepared a "chimera" embryo composed of two different species that are histologically distinguishable from each other in the "short-term" lineage-tracing experiments. For example, the chimera obtained from closely related but different species, *X. laevis* and *X. borealis*, can be used, since the nuclei of *X. laevis* and *X. borealis* demonstrate different staining (Tashiro et al., 2006). However, metamorphosed young frogs immunologically reject the allogeneic skin grafts from the other adult frogs, even among the same species (DiMarzo and Cohen, 1982; Nakamura et al., 1987; reviewed in Izutsu, 2009), so that it is difficult to employ the chimera system for the "long-term" cell-tracing during regeneration in the frogs (e.g., Lin et al., 2013). An major histocompatibility complex (MHC)-homozygous inbred strain of *X. laevis*, J strain (for history of the J strain, please refer to Session et al., 2016), exhibited no "long-term grafted skin rejection" even after metamorphosis (Tochinai and Katagiri, 1975). When the

hybrid frogs are produced by *X. laevis* J strain of eggs with sperms of other *X. laevis* (i.e., genetically GFP-labeled transgenic *X. laevis*), the hybrid that we named "JG"-frogs accepts a graft from "JJ"-metamorphosed individuals (J strain) without any immune rejection. Furthermore, we can easily distinguish GFP-positive cells of JG-hybrid from the cells of J strain by the GFP fluorescence or by the immunohistochemical method against GFP protein as in histological identification of *X. borealis* cells from *X. laevis* cells. In this combination (the JG-hybrid recipient and the J-strain donor), we can trace cell fate during the entire process of tissue regeneration.

Over the past two decades, development of a Tg technique using *X. laevis*, originally reported by Kroll and Amaya (1996), enabled us to genetically label the whole cells in the whole body with fluorescent proteins, such as GFP, that can be sensitively detected (reviewed in Ogino and Ochi, 2009). Reciprocal transplants between wild-type and Tg embryos allow us to label specific tissues in tadpoles (e.g., Gargioli and Slack, 2004), but again, immune rejection makes reciprocal transplants problematic after metamorphosis. Here we developed a novel method for tracing cell fate in skin regeneration more easily and clearly by using a Tg *X. laevis* line that ubiquitously expresses GFP. We prepared a JG-hybrid between the J strain and a transgenic *X. laevis* that ubiquitously expresses GFP and grafted tissues from J-strain donors to JG-hybrid recipients. Using this method, which allowed us to trace cell fate after metamorphosis without immune rejection, we found that cells from subcutaneous tissues contributed to skin regeneration, especially dermal regeneration, in the *X. laevis* froglet.

Results

Skin Over Subcutaneous Muscle Tissue Can Regenerate Scarlessly After Full-thickness Skin Excision

We previously reported that skin on the back (dorsal-trunk skin) and hindlimbs of a *X. laevis* froglet can almost completely regenerate the skin structure, including the dermis and secretion glands, after the removal of a square, full-thickness piece of skin including the dermis and epidermis (Yokoyama et al., 2011). Although we observed degradation of the subcutaneous tissue (musculature) under the wound, it was sometimes difficult to recognize the boundary between the dermis and the musculature because we used hematoxylin and eosin (HE), which stains both the dermal layer and the underlying musculature a pink color. In the present study, we used a different histological staining technique to confirm the boundary between the dermis and musculature, and to observe the regeneration process of the dermal layer as opposed to muscle regeneration. We also compared the histological transition of the wound-healing process between the back, forelimb, and head. In this study, we used Elastica van Gieson (EVG) and Alcian blue (AB) to stain the dermis a vivid red and stain the underlying musculature beige (Fig. 1C). This differential staining made it easier to distinguish the dermis from the subcutaneous tissue, which is primarily muscle in the *X. laevis* froglet limbs and back (Figs. 1C, 2C; Yokoyama et al., 2011).

We created a skin wound on the trunk by excising a 1.5–2.0-mm square piece that included the dermis (Fig. 1A,B). In the intact skin of the *X. laevis* froglet, the attachment between the skin and subcutaneous tissues is so fragile that they often separate during fixation and embedding for paraffin-embedded or frozen sections (Fig. 1C; note the space between the skin and
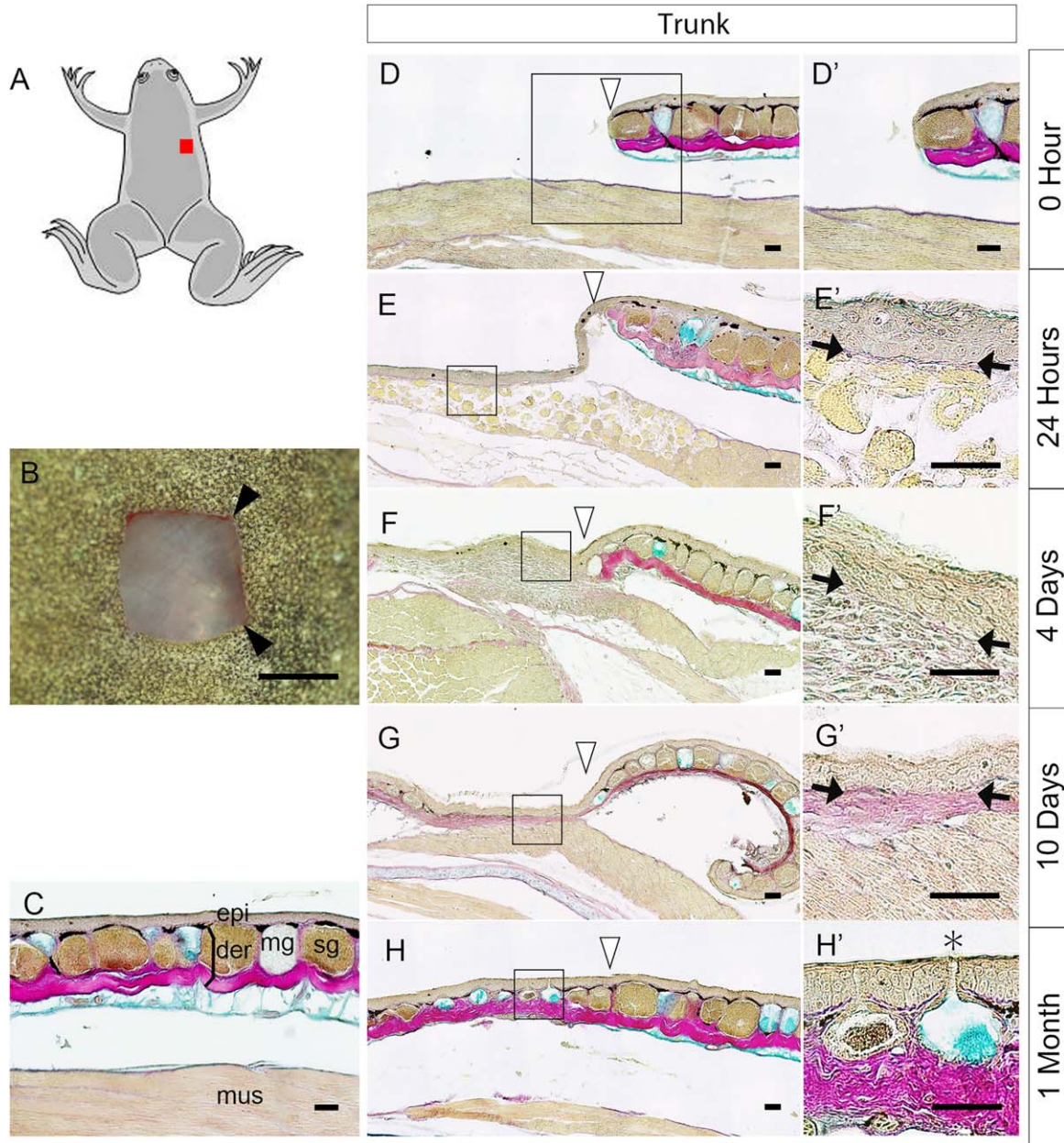
DEVELOPMENTAL DYNAMICS

Fig. 1. Trunk-skin regeneration and wound healing after excision. **A**: Illustration of a metamorphosed froglet; the red rectangle shows the location for skin excision. **B**: The skin wound immediately after excision. **C**: A section of intact trunk skin stained with Elastica van Gieson and Alcian blue. Epi, epidermis; der, dermis; mg, mucous gland; sg, serous gland; mus, muscle (n = 4). **D'–G'**: Magnified views of the rectangles in D–G. Time after incision: D,D', 0 hr (immediately after skin excision) (n = 4); E,E', 24 hr (n = 4); F, F', 4 days (n = 4); G,G' 10 days (n = 4); **H,H'**, 1 month after excision (n = 3). Black arrowheads (B) indicate the wound site. Open arrowheads (D–H) indicate the right-hand border of the wound. Black arrows (E'–G') indicate the basement membrane of the epidermis. Asterisk (H') indicates an exocrine gland duct. B: Bar = 1 mm. C–H,D'–H': Bar = 50 μm.

subcutaneous muscles). In intact skin, the dermal layer contains exocrine glands (mucous and serous glands; Fig. 1C). Because the skin is only loosely attached to the subcutaneous tissue, the skin piece can be excised without damaging the subcutaneous tissues, as shown in Figure 1B,D,D'. At 24 hr after skin removal, the entire wound was covered with dermis-free epidermis (Fig. 1E,E'), which we called wound epidermis, mirroring the initiation stage of limb regeneration (Yokoyama et al., 2011). We also observed that the subcutaneous myofibrillar organization was disrupted (Fig. 1E,E'). By 4 days after skin removal, there were many mononu-clear cells under the wound epidermis (Fig. 1F,F'). By 10 days

after skin removal, staining showed partially regenerated, inter-twined collagen bundles in the dermal layer (Fig. 1G,G'). Within 1 month, the skin had regenerated almost completely, including the dermis and secretion glands, without any scar tissue (Fig. 1H,H'). These results revealed that the regeneration of the dermal layer of the skin started between the epidermis and the subcuta-neous muscles prior to the regeneration of the secretion glands.

Next, to determine whether forelimb skin has the same regen-erative ability as hindlimb skin, we excised skin from the fore-limbs of *X. laevis* froglets. We removed a square piece of skin 1.5–2.0 mm on each side from the dorsal forelimb stylopod
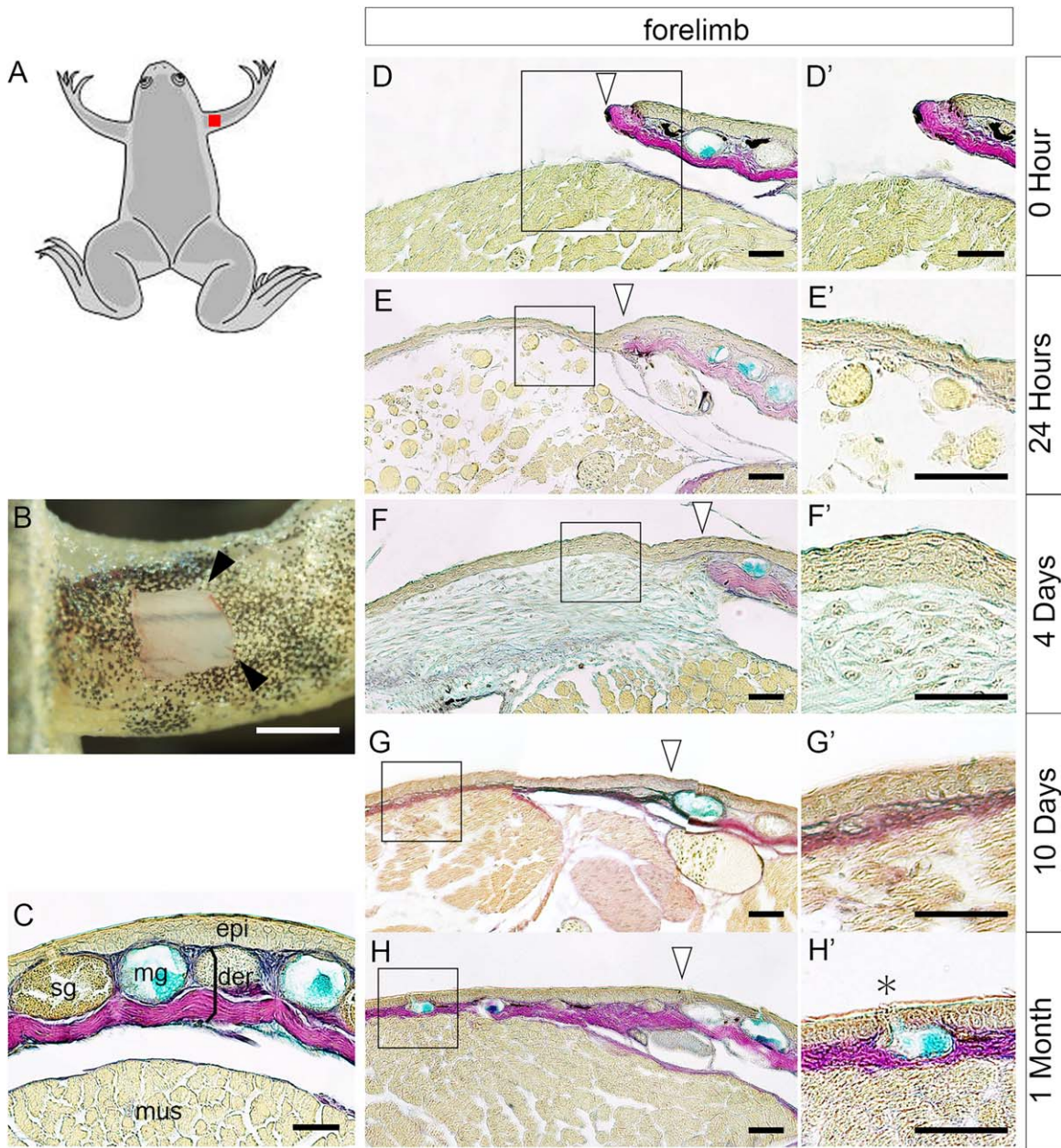
Fig. 2. Forelimb-skin regeneration and wound healing after excision. **A**: Illustration of a metamorphosed froglet; the red rectangle shows the location for skin excision. **B**: The skin wound immediately after excision. **C**: Intact forelimb skin stained with Elastica van Gieson and Alcian blue. Epi, epidermis; der, dermis; mg, mucous gland; sg, serous gland; mus, muscle (n = 1). **D'–H'**: Magnified views of the rectangles in D–H. Time after incision: D,D', 0 hr (immediately after skin excision) (n = 2); E,E', 24 hr (n = 4), F,F', 4 days (n = 4), G,G', 10 days (n = 5); H,H', 1 month after excision (n = 4). Black arrowheads (B) indicate the wound site. Open arrowheads (D–H) indicate the right-hand border of the wound. Asterisk (H') indicates an exocrine gland duct. B: Bar = 1 mm. C–H, D'–H': Bar = 50 μm.

(Fig. 2A,B). We found that the forelimb skin was able to regenerate almost complete structures without scarring in the same time period as trunk or hindlimb skin (Fig. 2D–H,D'–H'), indicating an equal regenerative capacity.

Skin Overlying the Skull Can Regenerate Without Scarring After Full-thickness Skin Excision

To determine whether subcutaneous muscles are required for scarless skin regeneration in the *X. laevis* froglet, we excised skin from the dorsal-medial head region, where the skin overlies bone

(the skull). The metamorphosed froglet has a pair of eyes on the dorsal side of the head (Fig. 3A). Alizarin red staining suggested that the subcutaneous tissue at the dorsal head region, especially in the medial area between the eyes, was composed exclusively of bone (Fig. 3B). To confirm this finding, we stained sections across the eye level with EVG and AB (Fig. 3C,C',C"). In the medial area, the underlying tissue was exclusively bone (Fig. 3C'). In the lateral area, however, there were a few muscles, presumably ocular muscles, around each eye (Fig. 3C"). These observations indicated that there was no subcutaneous muscle in the dorsal-medial head region (rectangle in Fig. 3B).
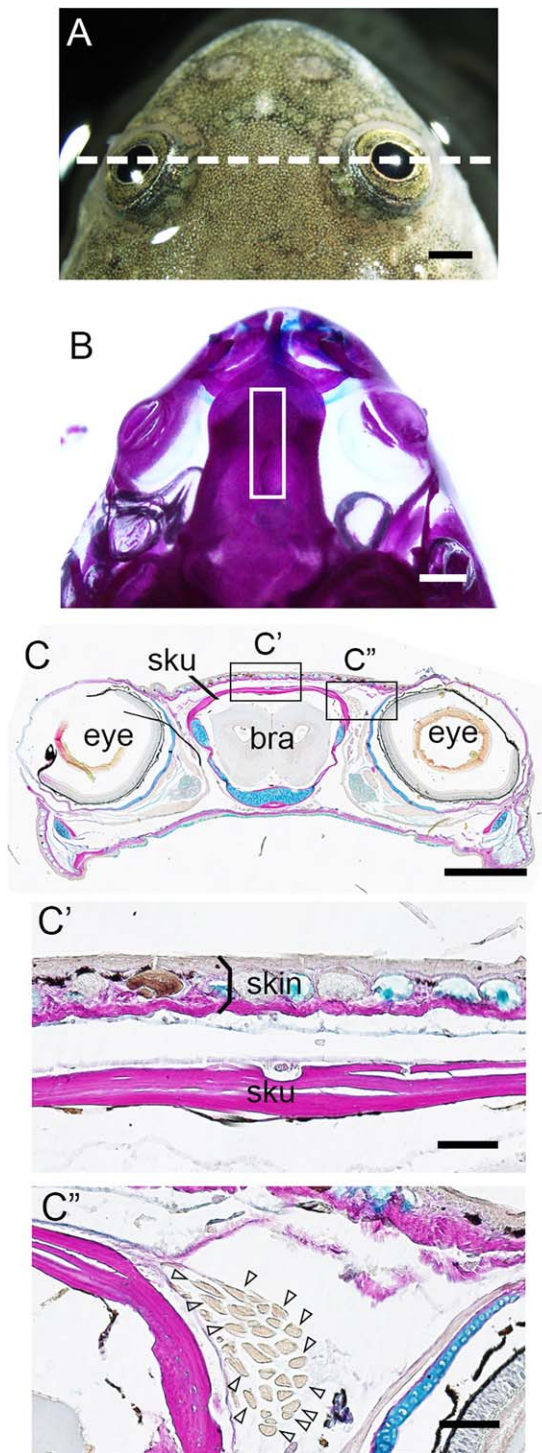
Fig. 3. Medial head skin overlies bone, not muscle. **A**: Brightfield view of the rostral portion of a *Xenopus laevis* froglet. **B**: Whole-mount bone staining of a froglet with Alizarin red. **C**: The head region was stained with Elastica van Gieson and Alcian blue and sectioned through the plane indicated by the dotted line in A. Bra, brain; sku, skull. **C',C":** Magnified views of the rectangles in C. The white rectangle in B indicates the medial-dorsal area of the head where the overlying skin was excised in Fig. 4. No subcutaneous muscles were observed in the medial head area C'. Open arrowheads (C") enclose ocular muscles. A–C: Bar = 1 mm. C',C": Bar = 100 µm.

For skin regeneration experiments in the head area, we chose a dorsal-medial location to avoid any influence from ocular muscles. We excised the skin, including the dermis, in a rectangular shape (0.5–1.0 mm on the mediolateral axis and 1.0–2.0 mm on the rostrocaudal axis) (Fig. 4A,B). The skin structure in the dorsal-medial head region, including the dermis, mucous glands, and serous glands, was identical to that in the trunk and limb regions (Fig. 4C). As with the skin on the back and limbs, there was a space between the skin and the subcutaneous bone in the dorsal-medial head region (Fig. 4C), and we were able to remove the skin without damaging the bone (Fig. 4D,D'). By 24 hr after skin removal, the entire wound was already covered with dermis-free wound epidermis (Fig. 4E,E'). Although there was no apparent disruption of the subcutaneous bone tissue below the wound, as was seen in the trunk and limb regions, mononuclear cells had accumulated between the wound epidermis and the bone (Fig. 4E,E'). By 4 days after skin removal, there were many mononuclear cells under the wound epidermis (Fig. 4F,F'), and by 10 days after skin removal, EVG staining showed partially regenerated, intertwined collagen bundles in the dermal layer (Fig. 4G,G'). Within 1 month, the skin was scar-free and almost completely regenerated, including the dermis and secretion glands, and a few mononuclear cells remained between the regenerated skin and subcutaneous bone (Fig. 4H,H'). Thus, the skin's regenerative ability and course of regeneration over time appeared to be similar in the head, trunk, and limbs. These results indicate that subcutaneous muscles are not essential for skin regeneration, and that mononuclear cells accumulate under the wound epidermis even when the underlying tissue is bone rather than muscle.

Blastema-like Cells With Activated *prx1* Limb Enhancer Accumulate Under the Wound Epidermis of Regenerating Trunk, Head, and Limb Skin

In a previous study, we found that blastema-like cells with activation of the limb-specific enhancer of the *prx1* (*prrx1*) gene, a marker for limb blastema cells, accumulate under the wound epidermis during skin regeneration in the *X. laevis* froglet (Yokoyama et al., 2011). We used the transgenic *X. laevis* line *Mprx1*-GFP to examine the activation of the *prx1* limb-specific enhancer (Suzuki et al., 2007) and found that it was activated in regenerating skin not only on the hindlimbs, but also on the trunk (Yokoyama et al., 2011); this was unexpected because the *prx1* limb enhancer is not activated in the dorsal trunk during normal development (Suzuki et al., 2007). In the present study, we examined whether the *prx1* limb enhancer was activated in regenerating skin on the head and forelimbs as well as on the trunk. As previously reported (Yokoyama et al., 2011), blastema-like cells with activated *prx1* limb enhancer were apparent in the wound area on the trunk 4 days after skin removal (Fig. 5A,B), while there were few GFP-positive cells in intact, uninjured skin (Fig. 5C,D). At 4 days after skin removal, GFP-positive blastema-like cells were apparent in the forelimb (Fig. 5E,F) and head regions (Fig. 5I,J). Notably, most of the GFP-positive cells were not observed in the wound epidermis (the uppermost cell layers) but beneath it (compare Figs. 5A,B, 5E,F, and 5I,J, respectively). In contrast, there were few GFP-positive cells in the intact, uninjured skin on the forelimb (Fig. 5G,H) and head (Fig. 5K,L). These results suggest that similar blastema-like cells accumulate and
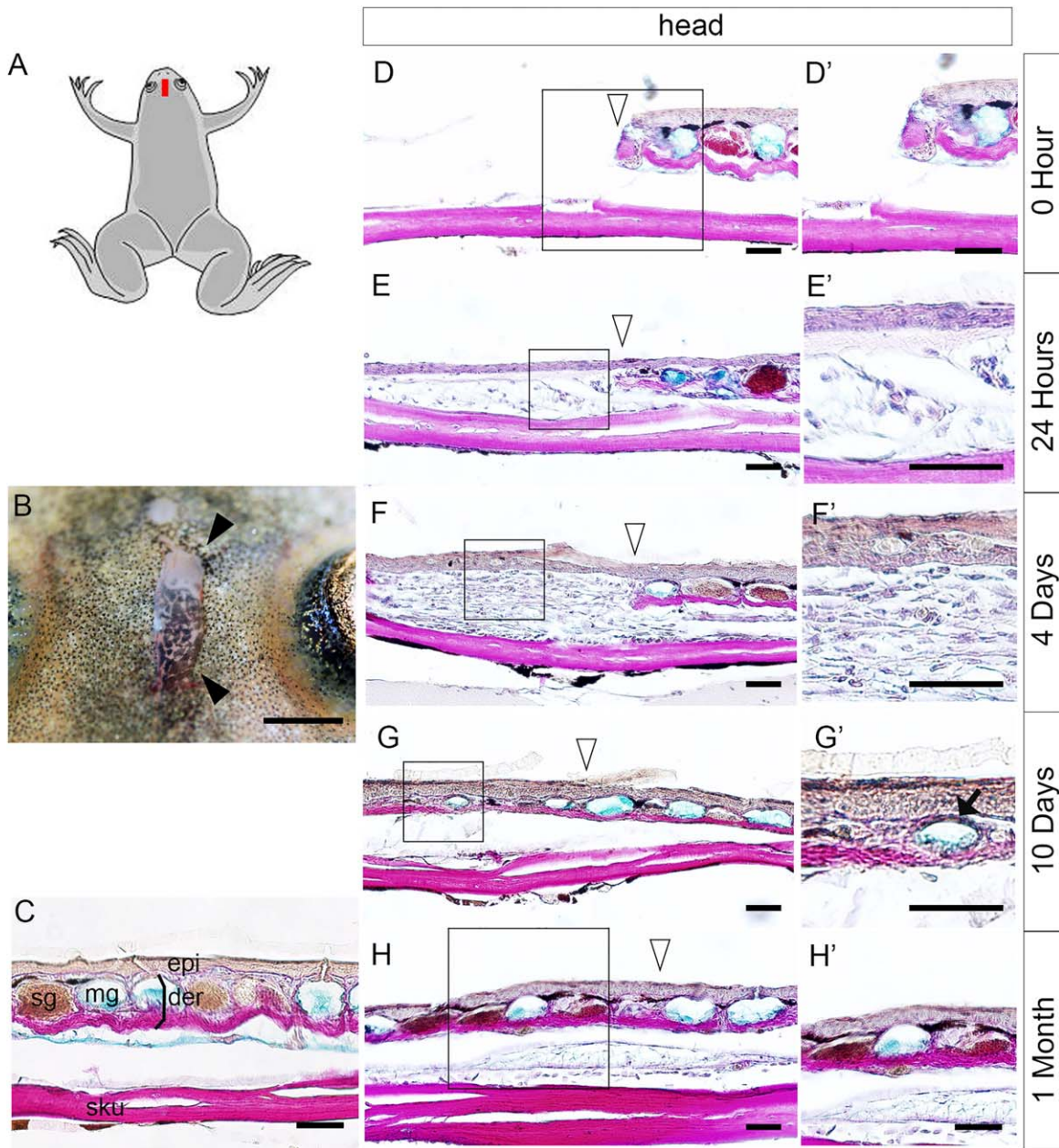
Fig. 4. Head-skin regeneration and wound healing after excision. **A**: Illustration of a metamorphosed froglet; the red rectangle shows the excision location. **B**: The skin wound immediately after excision. **C**: A section of intact head skin, stained with Elastica van Gieson and Alcian blue. Epi, epidermis; der, dermis; mg, mucous gland; sg, serous gland; sku, skull (n = 4). **D'–H'**: Magnified views of the rectangles in D–H. Time after excision: D, D', 0 hr (immediately after excision) (n = 3); E,E', 24 hr (n = 5); F,F', 4 days (n = 5); G,G', 10 days (n = 5); H,H', 1 month after excision (n = 4). Black arrowheads (B) indicate the wound site. Open arrowheads (D–H) indicate the right-hand border of the wound. Black arrow (G') indicates maturing secretion gland. B: Bar = 1 mm. C–H, D'–H': Bar = 50 μm.

contribute to scarless skin regeneration on the trunk, limb, and head regions.

Subcutaneous Tissue–derived Cells Contribute to Skin Regeneration in the *Xenopus laevis* Froglet

During skin regeneration in the trunk and limbs of the *X. laevis* froglet, subcutaneous tissues beneath the skin wound appeared disrupted, and there were blastema-like cells with activated *prx1* limb enhancer under the wound epidermis (Fig. 5; Yokoyama et al., 2011). In the *Mprx1*-GFP transgenic *X. laevis* froglet, GFP-

positive cells were often found in the disrupted subcutaneous tissues 4 days after skin excision (Fig. 5). Therefore, we speculated that the blastema-like cells that contribute to skin regeneration might come from the subcutaneous tissues. To test this possibility, we investigated the cellular origin of skin-regenerating cells by preparing a JG-hybrid and grafting skin from J-strain donors to JG-hybrid recipients to trace cell fate in the subcutaneous tissues (Fig. 6A). Skin grafting requires wide, flat areas of skin and was thus feasible on the trunk but not the limbs or head. We grafted dorsal back skin from a J-strain froglet to a JG-hybrid froglet (Fig. 6A[1–2]). Once the grafted skin was accepted by the
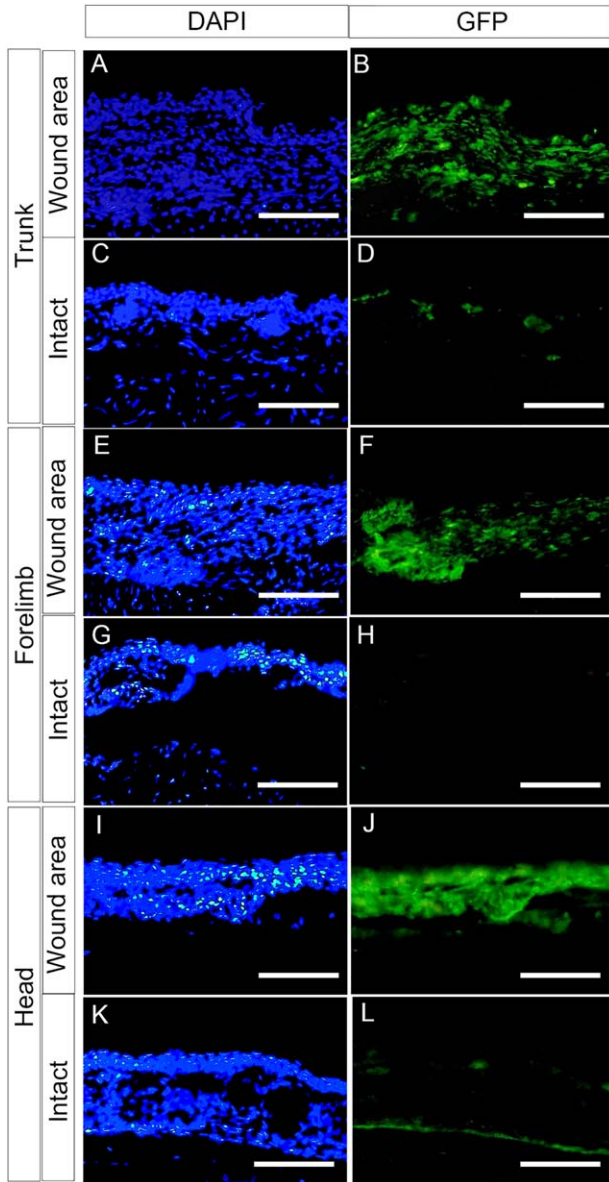
Fig. 5. The *prx1* enhancer was activated in all trunk, forelimb, and head-skin wound areas 4 days after skin excision in *Mprx1*-GFP froglets. Sections of regenerating and intact control skin were labeled with an anti-GFP antibody; nuclei were stained with DAPI. Immunostaining of regenerating skin around the original wound area (**A,B,E,F,I,J**) and intact (control) skin away from the wound area (**C,D,G,H,K,L**) in the same froglet. Little GFP was detected in the intact control skin (D,H,L), but robust staining for GFP was detected under the wound epidermis (B,F,J). Skin surface is up. Five of five and four of four individuals showed basically the same results in the trunk and forelimb, respectively. Two of four individuals showed robust staining for GFP in wound area of the head (J), but the rest showed relatively weaker staining for GFP. Bar = 100 µm.

host (recipient), the subcutaneous tissue but not the skin was labeled with GFP (Fig. 6A[2]). We then excised a square piece of skin inside the grafted area (Fig. 6A[3]) and examined the cell contribution from GFP-labeled subcutaneous tissues to the regenerating skin.

We first confirmed that the JG-hybrid froglet was ubiquitously labeled with GFP (Fig. 6C) and that the J-strain froglet was not labeled with GFP (Fig. 6B). The JG-hybrid host accepted skin
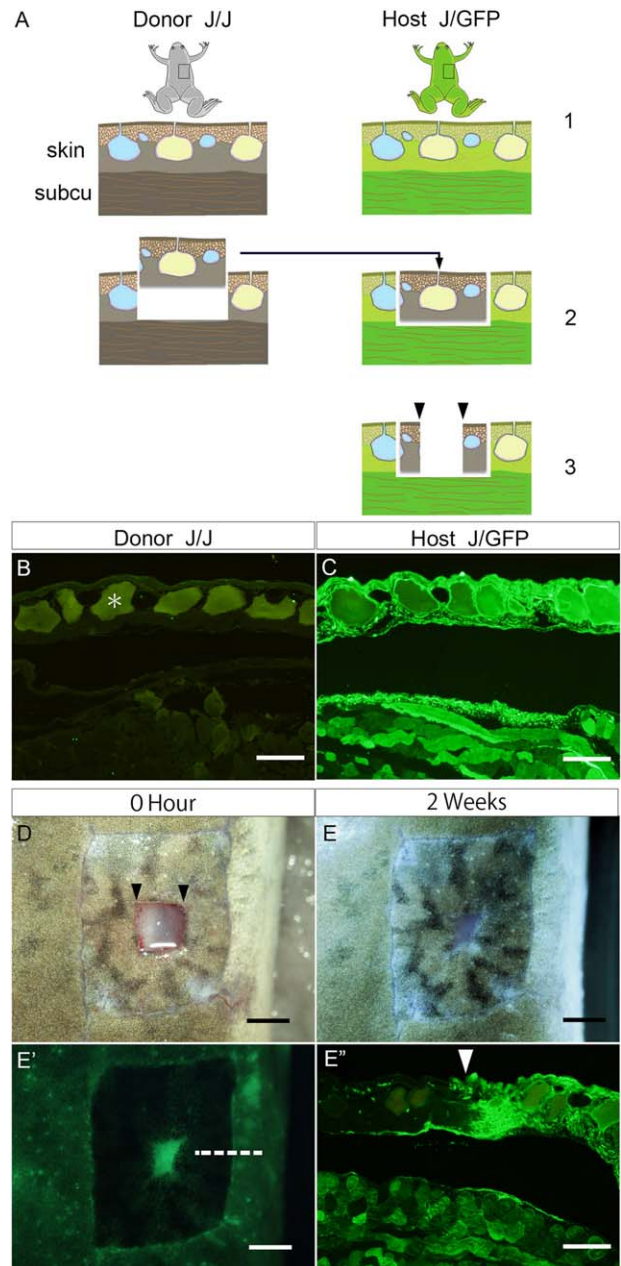

Fig. 6. Cell-fate tracing of subcutaneous tissues and regenerating skin in a froglet. **A**: Procedure for cell-fate analysis by skin grafting. The gray froglet represents a J-strain (J/J) individual; the green froglet represents a JG-hybrid (J/GFP) individual. 1: Skin and subcutaneous tissues are ubiquitously labeled with GFP in the J/GFP froglet. 2: A full-thickness skin piece was grafted from the J/J donor to the J/GFP recipient. 3: Once the grafted skin was accepted by the recipient, skin in the center of the graft, including the dermis, was excised. Subcu, subcutaneous tissues. **B**: Intact skin from a J-strain (n = 1) and (**C**) JG-hybrid (J/GFP) froglet (n = 1). **D**: Brightfield view of the skin wound in the graft area immediately after excision. **E,E'**: Brightfield (E) and GFP-fluorescence (E') views of the skin wound 2 weeks after injury. **E"**: The sample was sectioned through the plane indicated by the dotted line in E' and immunostained with an anti-GFP antibody. The grafted skin was rarely invaded by GFP-positive host-derived cells. Black arrowheads indicate the wound site; white arrowhead indicates the host-graft boundary. B,C,E": Bar = 200 µm. D,E,E': Bar = 2 mm.
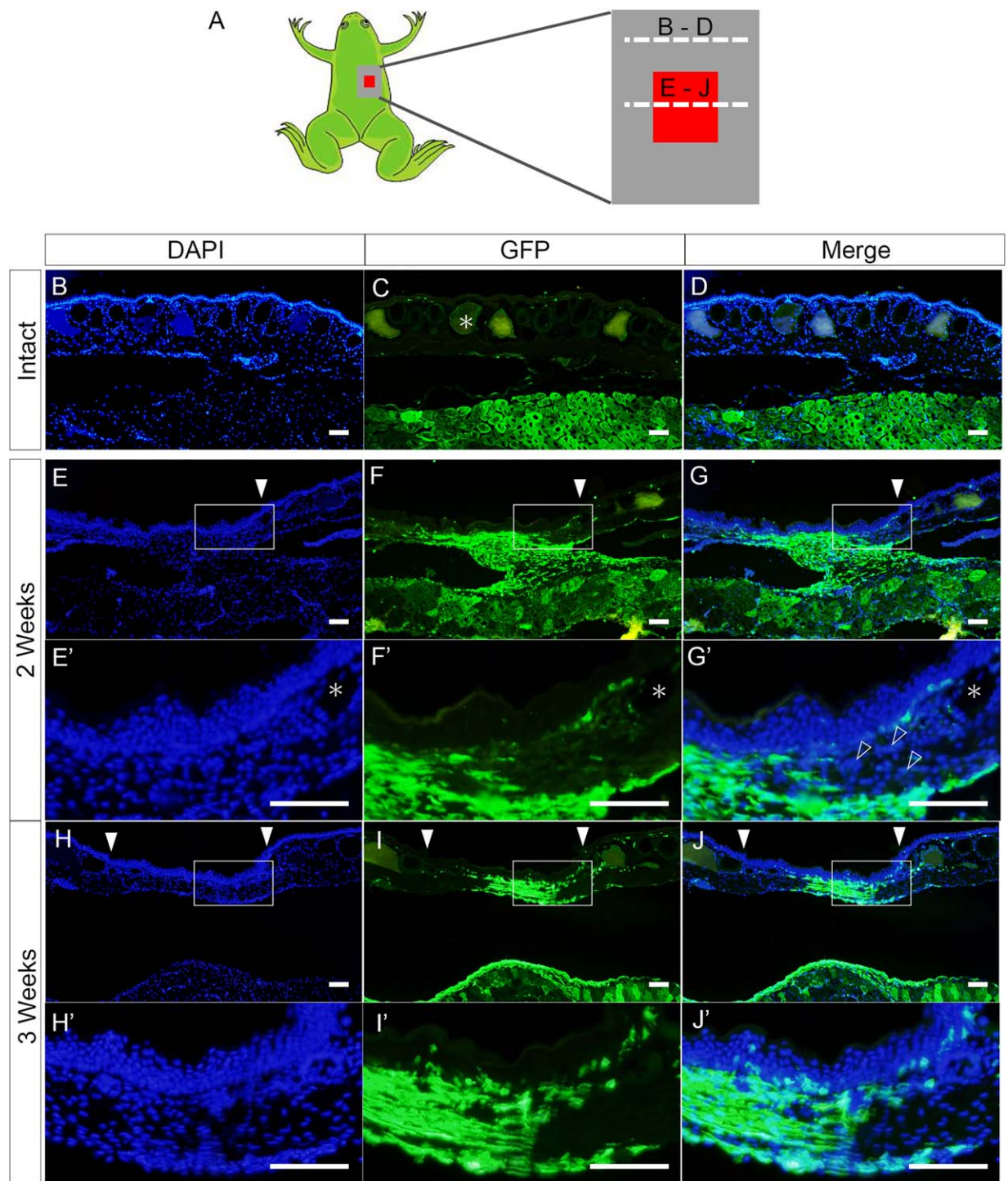
DEVELOPMENTAL DYNAMICS

Fig. 7. Cells derived from subcutaneous tissues contribute to skin regeneration. **A**: Illustration of a metamorphosed froglet indicating the transverse planes of sections shown as B-J and as E'-J'. Gray and red rectangles represent the grafted donor skin and excisional skin wound, respectively. **B–D**: Samples of intact skin regions were sectioned through the plane indicated by the dotted line as "B–D" in A. GFP-positive subcutaneous tissues were observed beneath the GFP-negative grafted skin. **E–J**: Samples of regenerating skin, including subcutaneous tissues, were sectioned through the plane indicated by the dotted line "E–J" at 2 or 3 weeks after skin excision. E–G: GFP-positive cells had accumulated underneath the GFP-negative wound epidermis at 2 weeks after skin injury (n = 4). Three of four individuals showed basically the same results. H–J: GFP-positive cells contributed to the regenerated skin, especially to the dermis in the center of the wound (n = 4). Four of four individuals showed basically the same results. Asterisks indicate secretion glands. White arrowheads (E–G) indicate the right-hand border of the wound. Pairs of white arrowheads (H–J) indicate the left- and right-hand borders of the wound. Open arrowheads indicate GFP-negative cells contributing to the dermis of the regenerating skin. Bar = 100 µm.

grafts from the J-strain donor froglet without immune rejection (Fig. 6D,E). There was a sharp boundary between the GFP-negative graft and the GFP-positive host tissues on whole-mount (Fig. 6E') and section (Fig. 6E") samples. Two weeks after a skin piece was excised from the grafted area (Fig. 6D), the wound appeared to be closing and regenerating (Fig. 6E,E'). As far as we observed, the skin pattern (coloration) of the regenerating region was not affected by the JG-hybrid host (data not shown). At 2 and 3 weeks after skin removal, we fixed and sectioned samples and examined the cell contributions by immunostaining (Fig. 7A). In intact skin away from the wound, GFP was present in the subcutaneous tissues, including the muscles, but not in the skin, and there was a space between the skin and the subcutaneous muscles (Fig. 7B–D). At 2 weeks after skin removal, GFP-positive cells derived from the subcutaneous tissues had migrated and accumulated under the wound epidermis and had bridged the wound epidermis and subcutaneous tissues in three of four samples (Fig. 7E–G). In regenerating skin within the wound, GFP-positive cells had contributed to skin tissues under the epidermis (presumably the dermal layers), but not to the wound epidermis itself (Fig. 7E'–G'). At 3 weeks after skin removal, the regenerated skin appeared to be separate from the subcutaneous tissues (Fig. 7H–J). The dermis had regenerated, and GFP-positive cells had contributed significantly to the regenerated dermis, especially in the center of the wound, in all four samples (Fig. 7H–J). Again, GFP-positive cells had contributed to the dermis but not the epidermis (Fig. 7H'–J'). These observations indicate that cells from subcutaneous tissues contribute to skin regeneration, especially to the regenerating dermis, in scarless skin regeneration in the *X. laevis* froglet.

Discussion

A *Xenopus laevis* Froglet Can Regenerate Scarless Skin Irrespective of Body Region or Type of Subcutaneous Tissue

Neither neonate nor adult mammals can completely regenerate skin; instead, a scar forms after skin is injured to the dermal layer (Ferguson and O'Kane, 2004; Gurtner et al., 2008; Stocum, 2012). Since *X. laevis* can regenerate its skin after a full-thickness skin wound as a metamorphosed young adult (froglet), *Xenopus* skin is a useful model for studying scarless skin regeneration as adults. Completion of the whole genome sequencing in *X. laevis* (Session et al., 2016) would facilitate direct and detailed comparison of *X. laevis* and mammals in skin wound healing and skin regeneration. One big advantage of amphibian models including *Xenopus* is that amphibians can regenerate an amputated limb (and other appendages) as well as injured skin through blastema formation, although *Xenopus* regenerates only a hypomorphic limb after metamorphosis (Dent 1962; reviewed by Suzuki et al., 2006). Thus, we can compare limb regeneration and skin regeneration in the same species. In axolotls, a skin wound on the side of a limb results in skin regeneration. However, this skin regeneration is stepped up to regeneration of an extra limb if the nerve axons are deviated to the wound site and a piece of skin is grafted from the opposite side of the limb (Endo et al., 2004). An extra limb can also be formed in a *X. laevis* froglet, although the formed accessary limb is hypomorphic (Mitogawa et al., 2014). Therefore, a skin-regeneration model in *Xenopus* would be useful for determining how skin regeneration is stepped up to limb

regeneration. Elucidation of this process would lead to the realization of regeneration of a three-dimensional organ such as a limb in mammals.

In mammals, the skin's ability to heal differs by body region. In adult humans, for example, the same size incision will form a larger scar on the deltoid and sternum of the chest than on the legs (Ferguson and O'Kane, 2004). In contrast, the *X. laevis* froglet was able to regenerate skin in all the areas we examined. Skin on the dorsal trunk (Fig. 1), forelimb (Fig. 2), head (Figs. 3 and 4), and hindlimb (Yokoyama et al., 2011) regenerated almost complete skin structures, including the dermis and secretion glands, without forming a recognizable scar. These observations were further supported by the finding that the *prx1* limb enhancer was strongly activated around the skin wound on the dorsal trunk, forelimb, and head in *Mprx1*-GFP transgenic froglets, while little activation was detected in the intact skin (Fig. 5). Since the *prx1* limb enhancer is activated in the scarless skin regeneration of the *Xenopus* froglet, but not in the scar-forming wound healing in adult mouse skin, we previously proposed that *prx1* enhancer activity might be a reliable marker for scarless skin regeneration (Yokoyama et al., 2011). Consistent with this idea, we found that cells with activated *prx1* limb enhancer contributed to scarless regeneration in the trunk, forelimb, and head (Fig. 5). Therefore, cells with activated *prx1* limb enhancer may be essential contributors to the scarless skin regeneration in amphibians. An intriguing question is whether the *prx1* gene product itself plays an important role in skin regeneration. Recent studies in mammals report that *prx1* regulates the stemness of adult neural stem cells (Shimozaki et al., 2013) and induces EMT (epithelial-mesenchymal transition) to confer migratory and invasive properties in embryo and cancer cells (Ocaña et al., 2012). Therefore, the *prx1* gene product may contribute to scarless skin regeneration by maintaining stem cells or regulating cell migration. It would be interesting to examine the role of endogenous *prx1* in skin regeneration by targeting the *prx1* gene by genome editing, since techniques for highly efficient gene targeting have recently become available in *Xenopus* (Nakayama et al., 2014; Sakane et al., 2014).

Activation of the *prx1* limb enhancer was detected under the wound epidermis after skin excision in the trunk, limbs, and head (Fig. 5), and the spatiotemporal pattern of enhancer activation overlapped with the distribution of mononuclear cells accumulating under the wound epidermis after skin excision in the trunk (Fig. 1), limbs (Fig. 2), and head (Fig. 4). The fact that the mouse *prx1* limb enhancer was activated in scarless skin regeneration in all of the examined body regions of the *Mprx1*-GFP froglet (Fig. 5) further suggests that all of the cis-regulatory elements required for *prx1* expression in scarless skin regeneration are conserved between the mouse and *Xenopus*. Determination of how the *prx1* limb enhancer is activated in a skin wound of mammals may lead to the realization of scarless skin regeneration in the future. While the function of the *prx1* gene product in skin regeneration is unclear, it is possible that skin regeneration in all of these regions (trunk, limbs, and head) involves common a mechanism (or mechanisms) that requires activation of the *prx1* limb enhancer. Our previous observation that cells with activated *prx1* limb enhancer were often surrounded by disrupted subcutaneous tissues, especially in the trunk and limbs (Yokoyama et al., 2011), led us to suspect that subcutaneous tissues contribute to skin regeneration after injury in *Xenopus*.

Cells Derived from Subcutaneous Tissues May Play Critical Roles in Scarless Skin Regeneration

Based on the observation that degrading subcutaneous tissues under the skin excision contain cells with *prx1* limb enhancer activation (Fig. 5), we previously hypothesized that cells derived from muscle, bone, and other subcutaneous tissues might contribute to skin regeneration in the *Xenopus* froglet, but we did not find any direct evidence of the role of subcutaneous tissues. In the present study, we invented a new method for tracing cell fate by GFP labeling without immune rejection using J-strain and JG-hybrid *X. laevis* froglets (Fig. 6). This long-lasting GFP labeling allows us to follow cell fate and distinguish cells from two closely related species without labor-intensive histological cell-marking methods such as differential nucleolar staining. Our method should be useful for analyzing cell fate in phenomena other than skin regeneration, so long as it can be used with a non-GFP-labeled donor and a genetically GFP-labeled recipient (tissues grafted from a JG-hybrid donor to a J-strain recipient will be immunologically rejected). Since several inbred *X. tropicalis* strains are being established (Igawa et al., 2015), this method should be applicable to *X. tropicalis* as well. Combining an inbred strain and a hybrid between the inbred strain and the transgenic line should prove to be a powerful tool for analyzing cell fates in *Xenopus* and in other biological resources.

Our skin-transplant experiment using J-strain and JG-hybrid froglets indicated that cells derived from subcutaneous tissues migrated to the wound and contributed to skin regeneration (Fig. 7). GFP-labeled cells derived from subcutaneous tissue contribute particularly to regenerating skin (dermis) in the central area of the original wound (Fig. 7I,I',J,J'). In contrast, there were few GFP-labeled cells at the periphery of the original wound, near the intact skin (Fig. 7I,J), probably because cells from the skin remaining around the wound contributed to regeneration at the wound edge. Among mammals, adult mice are exceptional in that they can regenerate hair follicles in the center of a wound after full-thickness skin excision; however, this happens only in wounds larger than a certain size (Ito et al., 2007). Cell migration and contracture from the peripheral skin around the wound may partially contribute to skin regeneration in the *Xenopus* froglet, and cells from subcutaneous tissues may be dispensable when the wound is relatively small. It would be intriguing to examine whether the cell contribution from subcutaneous tissues increases in a *Xenopus* froglet with a larger excision area, using the same skin transplant method between the J-strain and JG-hybrid froglets as shown in Fig. 6A. It would also be interesting to investigate the origin of the cells that contribute to skin regeneration by a comparative analysis of subcutaneous tissue–derived cells in *Xenopus* skin regeneration and hair-follicle regeneration in mice. When cells derived from subcutaneous tissues migrated to the central area of the original wound, these cells should have accumulated under the wound epidermis in the skin-transplant experiment for which results are shown in Figures 6 and 7. A previous study indicated that the wound epidermis derived from xenografted skin of an anuran amphibian (*Rana pipens*) can support and promote blastema formation of an axolotl limb (Carlson, 1982). Therefore, attraction and accumulation of blastema-like cells in skin regeneration may be mediated by a conserved molecular mechanism (or mechanisms) in the interaction of the wound epidermis and subcutaneous tissues among anuran and urodele amphibians.

To determine what type (or types) of cells in subcutaneous tissues contributes to skin regeneration in the *Xenopus* froglet, we experimented with skin transplants on the dorsal trunk, where most of the subcutaneous tissue is muscle. However, skin on the head can also regenerate without scarring, even though the underlying tissue is bone rather than muscle (Fig. 4). This raises two possibilities for contributing cells: One is that cells found in subcutaneous tissues common to the trunk, limb, and head, such as connective tissue, adipose tissue, vascular endothelial cells, pericytes, and Schwann cells of the peripheral nervous system, can contribute to skin regeneration. The second possibility is that several cell types from various subcutaneous tissues can contribute to skin regeneration. For example, muscle, satellite cells, or muscular fascia in subcutaneous tissues might contribute to skin regeneration in the trunk and limb regions, while subcutaneous periskeletal cells might contribute to skin regeneration in the head region. Unfortunately, the skin-transplant experiment shown in Figure 6A requires a large, flat area of skin, which is found only in the dorsal trunk. Thus, our current experimental technique cannot be used to elucidate the cellular contribution of subcutaneous tissues to skin regeneration on the head, where the skin curves over short distances. In any case, the next important task is to elucidate the precise cell type (or types) in subcutaneous tissues that contributes to scarless skin regeneration in amphibians. We believe that the next big question in an amphibian model for skin regeneration is the origin and identity of subcutaneous tissue–derived cells contributing to skin regeneration. Once this question is answered, we can examine whether their counterparts reside in subcutaneous tissues of mammals or not, providing insights into the reason why mammals cannot regenerate skin and why a skin wound results in scar formation. In this context, however, it is still very difficult to predict whether subcutaneous muscles actually contribute cells to skin regeneration in the *Xenopus* froglet, because muscle contribution to limb regeneration differs depending on species, even within urodele amphibians. Myofibers in the limb stump dedifferentiate and contribute significantly to limb regeneration in a newt (*Notophthalmus viridescens*), while myofibers do not contribute to limb regeneration in the axolotl (*A. mexicanum*) (Sandoval-Guzmán et al., 2014). To meet this challenge, techniques for analyzing cell fate at the single-cell level are needed. Single-cell labeling by infrared laser irradiation with the IR-LEGO (infrared laser–evoked gene operator) is applicable to amphibians, and although the target cell is labeled for only a brief period (Hayashi et al., 2014a; Kawasumi-Kita et al., 2015), the technique might still be useful for tracing cell fates in subcutaneous tissues. More recently, clonal analysis of cell fate with live monitoring using a Cre-loxP system (such as Brainbow) has revealed cell-migration behavior and cell contributions in appendage regeneration in axolotls (Currie et al., 2016) and Zebrafish (Tornini et al., 2016). If applicable in a skin-regeneration system, such a live-monitoring system would be a powerful method for analyzing the precise cell contributions from subcutaneous tissues to skin regeneration. In mammals, at least part of the fibroblast population in granulation tissue is derived from subcutaneous tissues (Ham and Cormack, 1979). Elucidating the origin of subcutaneous cells that contribute to skin regeneration and further comparing skin regeneration in amphibians and mammals (e.g., comparing the subcutaneous tissue–derived cells that contribute to skin regeneration in amphibians with fibroblasts that contribute to scar formation in mammals) would provide insight into the factors that switch

DEVELOPMENTAL DYNAMICS

wound healing from scar formation to regeneration or vice versa. Such comparative approaches will, we hope, lead to the realization of scarless skin regeneration in mammals, including humans.

Experimental Procedures

Animals and Preparation of JG-hybrid and *Mprx1*-GFP Transgenic Frogs

Adult frogs from an MHC-homozygous inbred J strain of *X. laevis* were obtained from a domestic animal vendor, Watanabe Zoushoku. The GFP transgenic line, called G-line, was obtained from the transgenic animals containing *gfp* gene under the control of *Xenopus* heat shock promoter (hsp70) produced by a nuclear transplantation technique using wild-type *X. laevis* (Mukaigasa et al., 2009). The original plasmid for the transgenesis is pHS1/EGFP described in Michiue and Asashima (2005). The partially inbred F4 G-line was obtained by hormone-induced mating of a female with a male, which are carefully selected as the strongest GFP-expressing individuals among siblings of F3 G-line. F2 and F1 G-lines were produced by mating of a female with a male in the same manner as above. Therefore, all embryos of F4 G-line represent ubiquitous GFP expression uniformly after the heat-shock treatment, suggesting that the F4 G-line is almost constant. JG-hybrid was obtained by mating with a sexually matured female of F4 G-line with a J-strain male frog in our laboratory. We randomly picked up a few representative individuals of the JG-hybrid and confirmed that they expressed ubiquitously GFP after whole-body heat-shock treatment at stage 59 (Nieuwkoop and Faber, 1994), showing that hsp70-GFP transgene are inherited derived from a parent. These JG-hybrid animals were used as hosts in this study, so that they are enabled to accept the graft from J strain and also to label the host cells with GFP. *Mprx1*-GFP F0, F1, and F2 Tg *X. laevis* were prepared as previously reported (Suzuki et al., 2007). For skin-wound experiments, we used froglets from the *Mprx1*-GFP F3 Tg *X. laevis* line, which was obtained by crossing sexually mature *Mprx1*-GFP F2 frogs with wild-type frogs. Wild-type froglets were purchased from Watanabe Zoushoku and Hamamatsu Seibutsu Kyozai. Tadpoles and froglets were reared at 23 °C–25 °C in dechlorinated tap water. The operated froglets were kept in a rearing container, at a maximum density of two froglets per liter. The rearing containers were cleaned daily, and the tadpoles were fed powdered barley grass (Odani Kokufun, Kouchi, Japan). At stage 58, feeding was discontinued until metamorphosis was complete. After metamorphosis, the froglets were fed dried *Tubifex* every other day. When skin samples were collected for skin grafting, histological analysis, or immunohistochemistry, the froglets were euthanized with 0.05% ethyl-3-aminobenzoate (Tokyo Chemical Industry, Tokyo, Japan) dissolved in Holtfreter's solution. We used wild-type and *Mprx1*-GFP F3 Tg froglets that have a snout-vent length of approximate 20 mm for skin-wound experiments. For skin-grafting experiments, we used J- and JG-hybrid froglets that have a snout-vent length of approximate 40 mm because skin-grafting experiment requires a wide and flat area of skin. All animal care and experimentation procedures were conducted in accordance with the guidelines of the committees for animal care and use for Tohoku University (2015LsA-023) and Hirosaki University (A15003, A15003-1).

Wounding Procedure and Skin Grafting

For wounding or skin grafting, froglets were anesthetized with 0.05% ethyl-3-aminobenzoate dissolved in Holtfreter's solution. The wounding procedure was as described in Suzuki et al. (2005) and Yokoyama et al. (2011) with slight modifications. A patch of skin was pinched with forceps, and a square piece (1.0–2.0 mm on a side) of skin including the dermis was removed with microdissection scissors, without damaging the underlying muscle (forelimb and back) or skull (head). For skin grafting, a square piece (12 mm on a side) of full-thickness skin was excised from the dorsal trunk of the euthanized J-strain donor froglet and kept in a 1:1 mixture of 0.1X MBS and Steinburg's solution at 4 °C for up to 10 min, until the recipient JG-hybrid froglet was anesthetized. Subsequently, a square piece (10 mm on a side) of the full-thickness dorsal-trunk skin was excised from the recipient, the cutaneous graft from the J-strain donor was trimmed to fit its prepared bed, and the properly orientated (left-right and rostrocaudal) skin graft was placed on the recipient. The four corners of the grafted skin were sutured to the recipient skin using a microsurgery needle with nylon thread (non-sterilized practice suture set, NTDY019, Kono Seisakusho, Japan). We assigned the donor/recipient pairs for skin grafting by similar body lengths. After skin grafting, animals were reared at 23 °C–25 °C in dechlorinated tap water. The operated froglets were kept in a rearing container, at a maximum density of two froglets per liter as mentioned above. One week after skin grafting, froglets on which the grafted area was obviously inflamed or the grafted skin had detached were removed from the experiment. Two weeks after skin grafting, we confirmed that the grafted skin was well accepted by the recipient froglet. Subsequently, a wound was created by excising a square piece (2 mm on a side) of full-thickness skin from the center of the graft.

EVG and AB Staining

For histological analysis, intact skin-piece samples and skin-piece samples that included the skin-wound area were excised and fixed in Bouin's fixative. For decalcification, samples were immersed in Morse's solution (22.5% formic acid, 10% sodium citrate) for 1 night (trunk and forelimb samples) or for 3–4 days (head samples). The fixed samples were washed with saturated Li_2CO_3 dissolved in 70% ethanol and then dehydrated with ethanol and cleared with xylene. The samples were embedded in paraffin, sectioned at 10 μm with a microtome, mounted on MAS-coated glass slides (Matsunami Glass Ind., Ltd.), washed with xylene to remove paraffin, and rehydrated with 70% ethanol. The sections were stained with Maeda's Resorcin-Fuchsin Solution (Muto Pure Chemicals Co., Ltd.) for 30–40 min to visualize elastic fibers, then immersed in 100% ethanol for 10 sec and washed with tap water followed by deionized water. Droplets of Weigert's Iron Hematoxylin Staining Solution (Wako Pure Chemical Industries, Ltd.) were mounted on dried sections, and the mounted sections were incubated 3–5 min to stain the nuclei. Subsequently, sections were washed with tap water, immersed in 70% ethanol with 1% HCl for 10 sec, and washed again with tap water followed by deionized water. Nuclear staining was confirmed, and the sections were stained in 1% AB (8GX) dissolved in deionized water (pH 2.5) for 10–15 min, washed twice with tap water, and washed once with deionized water. Droplets of van Gieson solution (picric acid, saturated : acid Fuchsin = 20:3) were placed on

mounted sections and incubated for 3–5 min to stain muscles, collagen fibers, and bone, after which the sections were washed with water, progressively dehydrated with 70%, 90%, and 100% ethanol, and cleared in xylene. Finally, the sections were sealed with EUKITT mounting medium (O. Kindler and ORSAtec). When the staining was complete, elastic fibers were dark purple (Resorcin-Fuchsin), nuclei were dark brown (iron hematoxylin), collagen fibers and bone were red (acid Fuchsin), muscle fibers were beige (picric acid), and cartilage and mucous were blue (AB). Each histological analysis by the EVG and AB staining of skin samples after excisional skin injury in the various regions (trunk, forelimb, and head) was repeated two to five times using different froglets.

Alizarin Red Staining

Whole-mount bone staining with Alizarin red was as previously reported (Grandel and Schulte-Merker, 1998; Hayashi et al., 2014b) with slight modifications. Samples were fixed with 4% paraformaldehyde/phosphate-buffered saline (PBS) for 4–5 days at 4 °C. The fixed samples were washed with PBS, dehydrated with ethanol/PBS, rehydrated with deionized water, and treated overnight with 5 mg/ml trypsin (BD Difco, 215240) in 30% saturated NaB_4O_7/70% water at 37 °C. To stain bone, samples were incubated in 4% Alizarin red (Sigma, A5533) saturated with ethanol/0.5% KOH at room temperature overnight, then washed with 0.5% KOH and bleached in 0.6% H_2O_2/1% KOH under strong light for 10 min at room temperature. Finally, samples were transferred to 87% glycerol via an ascending series of 0.5% KOH and 87% glycerol (10:1, 4:1, 5:2, 5:3, and 5:4, observed, and stored. Each Alizarin red staining experiment was repeated twice using different froglets.

Cell Tracing

To visualize cells derived from JG-hybrid Tg individuals, froglets were heat-shocked in 34 °C water for 30 min as described by Beck et al. (2003), and the induced GFP fluorescence was examined under a fluorescence-dissecting microscope 6 hr later. The froglets were subsequently euthanized with 0.05% ethyl-3-aminobenzoate. Samples of grafted skin and subcutaneous tissues were excised with a surgical blade or microdissection scissors and were immediately fixed with 4% paraformaldehyde/PBS for 2 hr at 4 °C. Cells derived from JG-hybrid froglets were visualized by immunostaining with an anti-GFP antibody.

Immunohistochemistry

Samples were immunostained as described by Suzuki et al. (2007). To visualize GFP protein in cells in JG-hybrid Tg froglets, or in hosts with a graft from a JG-hybrid Tg froglet, the froglets were heat-shocked 6 hr prior to fixation as described in the preceding paragraph. Samples were fixed with 4% paraformaldehyde/PBS for 2 hr at 4 °C and sectioned at 10 μm by cryostat. A rabbit anti-GFP antibody (Invitrogen, A-6455; 1:500) and goat anti-rabbit IgG Alexa 488–conjugated antibody (Molecular Probes, A11034; 1:500) were used as primary and secondary antibodies. Alternatively, a rat anti-GFP antibody (Nacalai Tesque, GF090R; 1:1000) and anti-rat IgG Alexa 488–conjugated antibody (A11006; 1:500) were used as primary and secondary antibodies as previously described (Suzuki et al., 2005; Yokoyama et al., 2011). Immunostaining of *Mprx1*-GFP froglet samples after excisional skin injury (trunk, forelimb, and head regions) was repeated at least four to five times using different froglets. Immunostaining of chimeric samples of J-strain recipients and JG-hybrid donor tissues was performed 2 weeks and 3 weeks after excisional skin injury and was repeated four times using different froglets.

References

Agata K, Inoue T. 2012. Survey of the differences between regenerative and non-regenerative animals. Dev Growth Differ 54:143–152.

Beck CW, Christen B, Slack JM. 2003. Molecular pathways needed for regeneration of spinal cord and muscle in a vertebrate. Dev Cell 5:429–439.

Bertolotti E, Malagoli D, Franchini A. 2013. Skin wound healing in different aged *Xenopus laevis*. J Morphol 274:956–964.

Brockes JP. 1997. Amphibian limb regeneration: rebuilding a complex structure. Science 276:81–87.

Brockes JP, Kumar A. 2005. Appendage regeneration in adult vertebrates and implications for regenerative medicine. Science 310:1919–1923.

Broughton G 2nd, Janis JE, Attinger CE. 2006. The basic science of wound healing. Plast Reconstr Surg 117:12S–34S.

Carlson BM. 1982. The regeneration of axolotl limbs covered by frog skin. Dev Biol. 90:435–440.

Currie JD, Kawaguchi A, Traspas RM, Schuez M, Chara O, Tanaka EM. 2016. Live Imaging of Axolotl Digit Regeneration Reveals Spatiotemporal Choreography of Diverse Connective Tissue Progenitor Pools. Dev Cell 39:411–423.

Dent JN. 1962. Limb regeneration in larvae and metamorphosing individuals of the South African clawed toad. J Morphol 110:61–77.

DiMarzo SJ, Cohen N. 1982. Immunogenetic aspects of *in vivo* allotolerance induction during the ontogeny of *Xenopus laevis*. Immunogenetics 16:103–116.

Endo T, Bryant SV, Gardiner DM. 2004. A stepwise model system for limb regeneration. Dev Biol 270:135–145.

Ferguson MW, O'Kane S. 2004. Scar-free healing: from embryonic mechanisms to adult therapeutic intervention. Philos Trans R Soc Lond B Biol Sci 359:839–850.

Gabbiani G. 2003. The myofibroblast in wound healing and fibrocontractive diseases. J Pathol 200:500–503.

Gargioli C, Slack JM. 2004. Cell lineage tracing during Xenopus tail regeneration. Development 131:2669–2679.

Grandel H, Schulte-Merker S. 1998. The development of the paired fins in the zebrafish (Danio rerio). Mech Dev 79:99–120.

Gurtner GC, Werner S, Barrandon Y, Longaker MT. 2008. Wound repair and regeneration. Nature 453:314–321.

Ham AW, Cormack DH. 1979. The Integumentary System (The Skin and Its Appendages). In Histology, 8th edition. Philadelphia: JB Lippincott. p 614–644.

Hayashi S, Ochi H, Ogino H, Kawasumi A, Kamei Y, Tamura K, Yokoyama H. 2014a. Transcriptional regulators in the Hippo signaling pathway control organ growth in Xenopus tadpole tail regeneration. Dev Biol 396:31–41.

Hayashi S, Tamura K, Yokoyama H. 2014b. Yap1, transcription regulator in the Hippo signaling pathway, is required for Xenopus limb bud regeneration. Dev Biol 388:57–67.

Igawa T, Watanabe A, Suzuki A, Kashiwagi A, Kashiwagi K, Noble A, Guille M, Simpson DE, Horb ME, Fujii T, Sumida M. 2015. Inbreeding Ratio and Genetic Relationships among Strains of the Western Clawed Frog, Xenopus tropicalis. PLoS One 10:e0133963.

Ito M, Yang Z, Andl T, Cui C, Kim N, Millar SE, Cotsarelis G. 2007. Wnt-dependent de novo hair follicle regeneration in adult mouse skin after wounding. Nature 447:316–320.

Izutsu Y. 2009. The immune system is involved in Xenopus metamorphosis. Front Biosci 14:141–149.

Kawasumi-Kita A, Hayashi T, Kobayashi T, Nagayama C, Hayashi S, Kamei Y, Morishita Y, Takeuchi T, Tamura K, Yokoyama H. 2015. Application of local gene induction by infrared laser-mediated microscope and temperature stimulator to amphibian regeneration study. Dev Growth Differ 57:601–613.

Kroll KL, Amaya E. 1996. Transgenic Xenopus embryos from sperm nuclear transplantations reveal FGF signaling requirements during gastrulation. Development 122:3173–3183.

Levesque M, Villiard E, Roy S. 2010. Skin wound healing in axolotls: a scarless process. J Exp Zool B Mol Dev Evol 314:684–697.

Lin G, Chen Y, Slack JM. 2013. Imparting regenerative capacity to limbs by progenitor cell transplantation. Dev Cell 24:41–51.

Michiue T, Asashima M. 2005. Temporal and spatial manipulation of gene expression in Xenopus embryos by injection of heat shock promoter-containing plasmids. Dev Dyn 232:369–376.

Mitogawa K, Hirata A, Moriyasu M, Makanae A, Miura S, Endo T, Satoh A. 2014. Ectopic blastema induction by nerve deviation and skin wounding: a new regeneration model in Xenopus laevis. Regeneration 1:26–36.

Mukaigasa K, Hanasaki A, Maéno M, Fujii H, Hayashida S, Itoh M, Kobayashi M, Tochinai S, Hatta M, Iwabuchi K, Taira M, Onoé K, Izutsu Y. 2009. The keratin-related Ouroboros proteins function as immune antigens mediating tail regression in Xenopus metamorphosis. Proc Natl Acad Sci U S A 106:18309–18314.

Muneoka K, Holler-Dinsmore G, Bryant SV. 1986. Intrinsic control of regenerative loss in Xenopus laevis limbs. J Exp Zool 240:47–54.

Nakamura T, Maeno M, Tochinai S, Katagiri C. 1987. Tolerance induced by grafting semi-allogeneic adult skin to larval Xenopus laevis: possible involvement of specific suppressor cell activity. Differentiation 35:108–114.

Nakayama T, Blitz IL, Fish MB, Odeleye AO, Manohar S, Cho KW, Grainger RM. 2014. Cas9-based genome editing in Xenopus tropicalis. Methods Enzymol 546:355–375.

Nieuwkoop PD, Faber J. 1994. Normal Table of Xenopus laevis (Daudin). New York: Garland Publishing. 282 p.

Norris RA, Scott KK, Moore CS, Stetten G, Brown CR, Jabs EW, Wulfsberg EA, Yu J, Kern MJ. 2000. Human PRRX1 and PRRX2 genes: cloning, expression, genomic localization, and exclusion as disease genes for Nager syndrome. Mamm Genome 11:1000–1005.

Ocaña OH, Córcoles R, Fabra A, Moreno-Bueno G, Acloque H, Vega S, Barrallo-Gimeno A, Cano A, Nieto MA. 2012. Metastatic colonization requires the repression of the epithelial-mesenchymal transition inducer Prrx1. Cancer Cell 22:709–724.

Ogino H, Ochi H. 2009. Resources and transgenesis techniques for functional genomics in Xenopus. Dev Growth Differ 51:387–401.

Pietsch P, Webber RH. 1965. Innervation and regeneration in orbitally transplanted limbs of Amblystoma larvae. Anat Rec 152:439–450.

Sakane Y, Sakuma T, Kashiwagi K, Kashiwagi A, Yamamoto T, Suzuki KT. 2014. Targeted mutagenesis of multiple and paralogous genes in Xenopus laevis using two pairs of transcription activator-like effector nucleases. Dev Growth Differ 56:108–114.

Sandoval-Guzmán T, Wang H, Khattak S, Schuez M, Roensch K, Nacu E, Tazaki A, Joven A, Tanaka EM, Simon A. 2014. Fundamental differences in dedifferentiation and stem cell recruitment during skeletal muscle regeneration in two salamander species. Cell Stem Cell 14:174–187.

Satoh A, Gardiner DM, Bryant SV, Endo T. 2007. Nerve-induced ectopic limb blastemas in the Axolotl are equivalent to amputation-induced blastemas. Dev Biol 312:231–244.

Seifert AW, Kiama SG, Seifert MG, Goheen JR, Palmer TM, Maden M. 2012a. Skin shedding and tissue regeneration in African spiny mice (Acomys). Nature 489:561–565.

Seifert AW, Monaghan JR, Voss SR, Maden M. 2012b. Skin regeneration in adult axolotls: a blueprint for scar-free healing in vertebrates. PLoS One 7:e32875.

Session AM, Uno Y, Kwon T, Chapman JA, Toyoda A, Takahashi S, Fukui A, Hikosaka A, Suzuki A, Kondo M, van Heeringen SJ, Quigley I, Heinz S, Ogino H, Ochi H, Hellsten U, Lyons JB, Simakov O, Putnam N, Stites J, Kuroki Y, Tanaka T, Michiue T, Watanabe M, Bogdanovic O, Lister R, Georgiou G, Paranjpe SS, van Kruijsbergen I, Shu S, Carlson J, Kinoshita T, Ohta Y, Mawaribuchi S, Jenkins J, Grimwood J, Schmutz J, Mitros T, Mozaffari SV, Suzuki Y, Haramoto Y, Yamamoto TS, Takagi C, Heald R, Miller K, Haudenschild C, Kitzman J, Nakayama T, Izutsu Y, Robert J, Fortriede J, Burns K, Lotay V, Karimi K, Yasuoka Y, Dichmann DS, Flajnik MF, Houston DW, Shendure J, DuPasquier L, Vize PD, Zorn AM, Ito M, Marcotte EM, Wallingford JB, Ito Y, Asashima M, Ueno N, Matsuda Y, Veenstra GJ, Fujiyama A, Harland RM, Taira M, Rokhsar DS. 2016. Genome evolution in the allotetraploid frog Xenopus laevis. Nature 538:336–343.

Shimozaki K, Clemenson GD, Gage FH. 2013. Paired related homeobox protein 1 is a regulator of stemness in adult neural stem/progenitor cells. J Neurosci 33:4066–4075.

Stocum DL. 1968. The urodele limb regeneration blastema: a self-organizing system. I. Morphogenesis and differentiation of autografted whole and fractional blastemas. Dev Biol 18:457–480.

Stocum DL. 2012. Repair of Skin by Fibrosis. In: Regenerative Biology and Medicine, 2nd ed. London: Academic Press. p 21–42.

Stoick-Cooper CL, Moon RT, Weidinger G. 2007. Advances in signaling in vertebrate regeneration as a prelude to regenerative medicine. Genes Dev 21:1292–1315.

Straube WL, Tanaka EM. 2006. Reversibility of the differentiated state: regeneration in amphibians. Artif Organs 30:743–755.

Suzuki M, Satoh A, Ide H, Tamura K. 2005. Nerve-dependent and -independent events in blastema formation during Xenopus froglet limb regeneration. Dev Biol 286:361–375.

Suzuki M, Satoh A, Ide H, Tamura K. 2007. Transgenic Xenopus with prx1 limb enhancer reveals crucial contribution of MEK/ERK and PI3K/AKT pathways in blastema formation during limb regeneration. Dev Biol 304:675–686.

Suzuki M, Yakushiji N, Nakada Y, Satoh A, Ide H, Tamura K. 2006. Limb regeneration in Xenopus laevis froglet. Scientific World Journal 6 Suppl 1:26–37.

Tashiro S, Sedohara A, Asashima M, Izutsu Y, Maéno M. 2006. Characterization of myeloid cells derived from the anterior ventral mesoderm in the Xenopus laevis embryo. Dev Growth Differ 48:499–512.

Tochinai S, Katagiri C. 1975. Complete abrogation of immune response to skin allografts and rabbit erythrocytes in the early thymectomized Xenopus. Dev Growth Differ 17:383–394.

Tornini VA, Puliafito A, Slota LA, Thompson JD, Nachtrab G, Kaushik AL, Kapsimali M, Primo L, Di Talia S, Poss KD. 2016. Live Monitoring of Blastemal Cell Contributions during Appendage Regeneration. Curr Biol 26:2981–2991.

Yokoyama H. 2008. Initiation of limb regeneration: the critical steps for regenerative capacity. Dev Growth Differ 50:13–22.

Yokoyama H, Maruoka T, Aruga A, Amano T, Ohgo S, Shiroishi T, Tamura K. 2011. Prx-1 expression in Xenopus laevis scarless skin-wound healing and its resemblance to epimorphic regeneration. J Invest Dermatol 131:2477–2485.